

Semantics-Depth-Symbiosis: Deeply Coupled Semi-Supervised Learning of Semantics and Depth

Nitin Bansal¹, Pan Ji^{1*}, Junsong Yuan^{1,2}, and Yi Xu¹

¹ OPPO Research Centre, Palo Alto, 94303, USA

² University at Buffalo, State University of New York, 14260, USA

Abstract. Multi-task learning (MTL) paradigm focuses on jointly learning two or more tasks, aiming for significant improvement w.r.t model’s generalizability, performance, and training/inference memory footprint. The aforementioned benefits become ever so indispensable in the case of joint training for vision-related **dense** prediction tasks. In this work, we tackle the MTL problem of two dense tasks, *i.e.*, semantic segmentation and depth estimation, and present a novel attention module called Cross-Channel Attention Module (CCAM), which facilitates effective feature sharing along each channel between the two tasks, leading to mutual performance gain with a negligible increase in trainable parameters. In a true symbiotic spirit, we then formulate a novel data augmentation for the semantic segmentation task using predicted depth called AffineMix, and a simple depth augmentation using predicted semantics called ColorAug. Finally, we validate the performance gain of the proposed method on the Cityscapes dataset, which helps us achieve state-of-the-art results for a semi-supervised joint model based on depth and semantic segmentation.

Keywords: Semantic Segmentation, Cross-Channel Attention Module, AffineMix, ColorAug, Depth Estimation, Multi-task learning

1 Introduction

Convolutional Neural Networks (CNNs) [34] have helped achieve state-of-the-art results for a range of computer vision tasks including image classification [22], semantic segmentation [3, 4, 36, 45], and depth estimation [19]. Generally, each of these tasks is trained in isolation, assuming that inter-task features are largely independent. On the contrary, multiple works in the domain of MTL [42, 66, 79] point towards an inherent symbiotic relation between multiple tasks, where one task benefits from other *sibling tasks*. In [65], Standley *et al.* particularly point towards a synergy for training semantic segmentation and depth estimation tasks jointly. Many previous works such as [7, 24, 28, 31, 56] further validate the benefits of MTL by achieving better results. Most of the MTL model encourages parameter sharing [15, 23, 32, 46], to enforce task generalization and thus help us

* Corresponding author

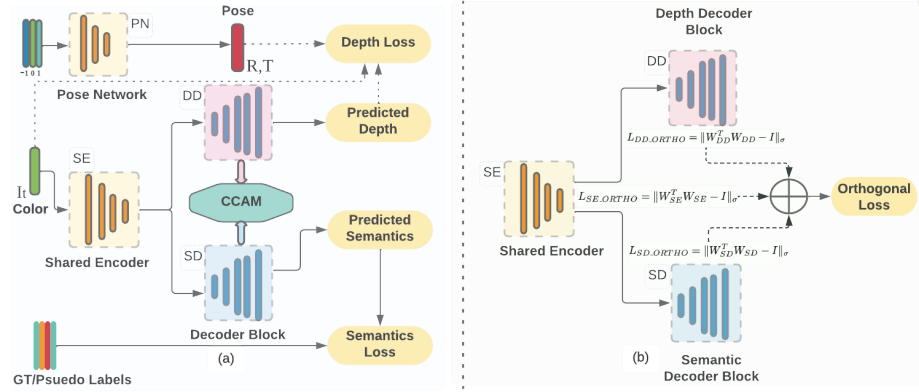


Fig. 1. (a): Block diagram of the complete multi-task model with semantics and depth losses. (b): Orthogonal regularization enforced on shared encoder(SE) along with depth(DD) and semantic decoder module(SD). W_{DD} , W_{SD} and W_{SE} represents the parameter of encoder and decoder blocks respectively, whereas $L_{DD.ORTHO}$, $L_{SD.ORTHO}$, $L_{SE.ORTHO}$ represents the orthogonal regularization loss for encoder and decoder blocks respectively.

overcome data sparsity problem, especially for tasks such as semantic segmentation and depth estimation, where obtaining perfect per-pixel annotations is both expensive and untenable in some scenarios. We thus follow a semi-supervised MTL training paradigm [33, 51, 67, 75] where semantic segmentation follows a semi-supervised setting and the depth sub-model is trained in a complete self-supervised manner similar to [19].

Architecture of MTL model is equally important as it decides how exactly the features between multiple tasks would be shared. As highlighted in [79], *what to share and how to share?* still remains an open question. We adopt a hybrid parameter sharing approach similar to what has been used in previous works [24, 76], which enforce a hard parameter sharing for encoding layers and a soft parameter sharing at decoder layers to facilitate both flexibility and inter-feature learn-ability. We propose a three pronged approach, where: (i) we facilitate effective feature transfer between the tasks using CCAM, during the MTL training phase; (ii) we formulate two new data augmentation techniques which enhance data diversity and reduce dataset bias in a symbiotic spirit and help improve both semantics and depth metrics; and (iii) we push towards learning independent parameters for depth and segmentation module through orthogonal regularization.

A few methods [7, 28, 31, 56] have tried to combine depth estimation and semantic segmentation training under one unified model, but they cannot guarantee an improvement for both tasks under a self-supervised or semi supervised setting, primarily because either they do not facilitate cross feature learning, or in case if they do, it is not as effective such that it benefits both the tasks. Moving away from previous works [24, 76], which overlook inter-channel interactions between tasks, the proposed CCAM module enforces dual attention on

intermediate depth and segmentation features over both spatial and channel dimensions, which enables us to estimate a degree-of-affinity between inter task channel-features as an intermediary score in an end-to-end framework, which is fully differentiable. Using CCAM, we can linearly weight the contribution of features of each task before sharing and thus encourage a more informed and reliable feature transfer between the tasks.

To improve semi-supervised semantic training, we propose an AffineMix data augmentation strategy, which aims to create new labeled images under a varied range of randomly selected depth scales. Under this scheme, randomly selected movable objects are projected over the same image, for a given depth scale. This unlocks another degree of freedom in data augmentation scheme, generating images which are not only close to original data distribution but also more diverse and class balanced. On the depth estimation end, we propose a simple yet effective data augmentation scheme called ColorAug, which establishes strong contrast between movable objects and adjacent regions, using intermediate semantics information. At last, we employ orthogonal regularization as an strategy to improve MTL training efficacy. We show that enforcing orthogonality to specific task modules helps learn more independent features across depth and semantics feature space, which eventually has a positive impact on both semantics and depth evaluation. To summarize our main contributions:

- We propose CCAM to estimate cross channel affinity scores between task features. This enables better inter-task feature transfer, resulting in a mutual performance gain.
- We formulate a dual data augmentation mechanism for both semantics and depth. Our method encourages diversity, class balance for semantic segmentation, and better region discrimination for depth estimation.
- We incorporate orthogonal regularization for depth and semantics with diminishing weighting, to facilitate better feature generalization and independence.

2 Related Work

2.1 Multi-Task Learning (MTL)

MTL [2] has been used across various tasks, as it improves generalization by transferring domain information of related tasks as an inductive bias. In the context of deep learning networks, it would translate to designing models which can learn a shared representation for multiple related tasks. Previous works such as [2, 23, 32, 41] have advocated for hard parameter sharing, where a certain parameters are shared by all the tasks, whereas [15, 46, 48] advocate soft sharing of parameters, where specific parameters are connected through a learnable link module. In our work we follow a hybrid approach, where in an encoder-decoder architecture we use a shared encoder but employ soft parameter sharing over the decoder module as shown in Fig 1(a). Previous works such as [15, 48, 59] are encoder focused, whereas [24, 76, 80] mainly focus on the decoder to facilitate

parameter sharing. Ours is an approach that gravitates more towards the latter category, but improves from the previous approach by enabling an efficient cross-task feature sharing mechanism using CCAM, which benefits both semantics and depth tasks. Furthermore, [43, 57] employ a residual adapter module, with an idea of dedicating a set of model’s parameters to each task in a MTL setup. In our approach, we do not use any such residual modules, but rather improve model’s shared representation capability through effective inter-task feature sharing. From optimization point of view, works such as [8, 21, 61] enforce task balancing by using gradient based multi-objective optimization. We in our experiment find little to no effect employing such regularization during our training and so refrain from using them in our setting. Finally there has been work [47, 64], which uses adversarial training and [29] which utilizes uncertainty during MTL training. Both of them have entirely different motivations compared to our work, and are not necessarily looking to better feature sharing, for two related tasks.

Trevor *et al.* [65] rightly identify semantic segmentation and depth estimation as complementary tasks, which seem to assist each other in a joint-training setup. A few other methods [7, 56] leverage semantic labels to jointly train on depth and semantics but mainly to improve on depth results. Marwin *et al.* [31] focus on improving depth results specifically for moving objects in a scene using the intermediary semantics information, whereas Jiao *et al.* [28] tackle long-tail distribution in depth prediction domain using semantics. Some of these models are not truly self-supervised for depth estimation or fail to jointly improve both tasks. Another approach in this particular context uses knowledge distillation [20, 76] from segmentation to guide depth estimation. Furthermore, some other methods [42, 76] exploit spatial attention [52, 70] for more effective cross-feature distillation and task related feature extraction. Most recently, Hoyer *et al.* [24] propose a joint training network, which has a feature sharing network between the task as proposed in [76]. Our experiments show that there is little impact on the result of depth and semantics upon inclusion/exclusion of this feature sharing module, suggesting ineffective feature transfer between the two tasks. Also [24] focuses only on improving semantic results using depth estimation procedure but not vice-versa. In contrast, CCAM as shown in Fig. 2, facilitates proportional sharing of features between depth and semantics across each channel. In a given multi-task setting containing two tasks, namely *Task A* and *Task B*, we estimate a cross-channel affinity score, which reflects how strongly each channel in *Task A* is related to all the channels in *Task B* and vice-versa. We then use the obtained score to scale each channel of *Task A* and *Task B* before feature sharing. Please refer to Sec.3.2 for more details.

2.2 Semi-supervised Semantic Segmentation

Deep convolutional neural network models [45, 62] have been the go-to network for both supervised and semi-supervised semantic segmentation tasks. Subsequent models have improved by leveraging multi-scale input images [5, 10, 12, 39, 40], which capture finer details using multi-scale features. Furthermore, there

have been models using feature pyramid spatial pooling [44, 81] and atrous convolutions [3, 4, 6, 36, 77], to further assist in better per-pixel feature learning and achieve state-of-the-art results. We choose an architecture similar to U-Net [58], details about which is in Sec. 4.

Semi-supervised semantic segmentation training makes use of an unlabeled set of data. Many approaches take image-level labels [35, 37, 73] and class activation maps [71, 82] as a weak supervision signal, which gives marginal assistance in a dense prediction task such as per-pixel segmentation. Methods based on consistency training [33, 51, 67, 75] use the idea that label space for unlabeled data should remain broadly unchanged after adding noise or perturbation to the input. Ouali *et al.* [54] use the same idea but apply perturbation on encoder features instead. Similarly, CutMix [78] vouches for stronger augmentations, where crops from input images and pseudo labels are used to generate additional training data. ClassMix [53] takes it a step forward by using pseudo labels to get a mix mask, which is then used in consistency training. Our proposed data augmentation is most similar to DepthMix [24], which uses the idea of ClassMix [53] but also maintains geometric consistency. Our approach differs from DepthMix [24] on three counts. Firstly, we propose a new data augmentation strategy which generates the pseudo labels for selected foreground classes under different randomly selected depth scales, keeping geometric consistency intact. Secondly, we mix foreground masks over the same image and not across the other images for a given batch. Lastly we only consider movable objects as part of the data augmentation with the idea of better handling the intrinsic data bias due to class imbalance. Please refer to Sec. 3.3 for more details.

2.3 Self-supervised Depth Estimation (SDE)

Depth estimation in the absence of per-pixel ground truth is a well-studied problem. The self-supervised model relies on minimizing the image reconstruction loss, for an input that could either be in stereo-pairs or in a monocular sequence format. Depth estimation under a stereo setting [16, 18, 19] mainly focuses on predicting pixel disparity between the pairs and enforcing a consistency between left and right views. In the monocular sequence scenario, methods such as [16, 18, 19, 26, 27, 68, 83, 84] minimize the photometric reprojection loss during the training phase using the predicted depth and pose. Our depth module largely follows Godard *et al.* [19]. In addition to the reprojection loss, we also enforce a per-pixel minimum appearance loss and auto-masking which further improves prediction for occluded and stationary pixels.

3 Proposed Method

In this section, we start with the basic architecture in Sec. 3.1. We then discuss in detail about building blocks of CCAM and how the resultant features are shared across different tasks in 3.2. Different strategies used for data augmentation for semi-supervised semantics and self-supervised depth network are subsequently

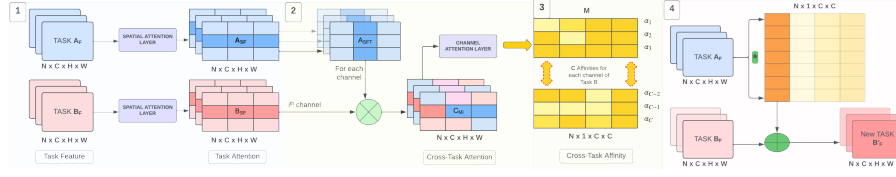


Fig. 2. Complete sub-blocks of Cross Channel Affinity Module (CCAM).

discussed in 3.3. We then briefly discuss the training strategy for depth and semantics part in 3.4 and 3.5 respectively. We conclude this section by presenting how we can effectively apply orthogonal regularization on semantics and depth modules together to further enhance model’s performance in 3.6.

3.1 Basic Architecture

For the multi-task training at hand, we follow soft or partial parameter sharing between the tasks. We use a shared encoder but separate decoders for semantics and depth tasks respectively as shown in Fig. 1. Apart from this, we use a separate encoder block for camera pose estimation, and an encoder pretrained on ImageNet [60] to calculate the feature distance loss, similar to [24]. The CCAM block (details in suppl. material) consists of mainly two sub-blocks, which mainly have convolutional, global average pooling and fully connected layers to compute spatial and cross-channel attention respectively. More specific details about different blocks are mentioned in Sec. 4.1, under network architecture.

3.2 Cross Attention Network Architecture

Under the domain of cross-task feature transfer, there have been mainly three approaches used as mentioned in [79]: (i) sharing a few initial layers to facilitate learning common features for complimentary tasks; (ii) using adversarial networks to learn common feature representation as in [63]; and (iii) learning different but related feature representations as presented in [49]. We take inspiration from these ideas to build a mechanism to effectively share features between semantics and depth modules. Particularly, Xu *et al.* [76] propose a multi-modal distillation block, which shares cross-task features through message passing. It simulates a gating mechanism as shown in Eq. (1) and (2), by leveraging the spatial attention maps of each individual features of all tasks, which then helps decide what features a given task would share with other tasks. Without loss of generality, suppose we train a total number of T tasks, and F_i^k denotes the i^{th} feature of the k^{th} task before message passing and $F_i^{o,k}$ after message passing. Xu *et al.* [76] define the message transfer as:

$$F_i^{o,k} = F_i^k + \sum_{t=1(\neq k)}^T G_i^k \odot (W_{t,k} \otimes F_i^t), \quad (1)$$

where \odot means element-wise product, \otimes represents convolution operation, and G_i^k denotes the gating matrix for i^{th} feature of the k^{th} task, which is given by:

$$G_i^k = \sigma(W_g^k \otimes F_i^k), \quad (2)$$

where W_g^k is a convolution block and σ denotes the sigmoid operator. We refer reader to [76] for more details regarding above message passing strategy. According to Eq. (1), it only shares cross-task features naively across the channel dimension. This indirectly implies that i^{th} channel-feature of F^k is only important to i^{th} channel-feature of F^l , which is not necessarily true in all scenarios. We overcome this major limitation by designing a module that calculates an affinity vector α_i , which gives an estimate about how the i^{th} channel of task F^k is related to any j^{th} channel of task F^l . As shown in Fig. 2, the entire process of building scores of inter-task channels can be subdivided into four sub-blocks, namely, **1**, **2**, **3**, **4**. Since in our case we are dealing with two tasks, we denote them as Task A and Task B, and their intermediate features are represented by A_F and B_F respectively, where $A_F, B_F \in \mathbb{R}^{N \times C \times H \times W}$.

CCAM Sub-block 1: We start with sub-block 1, where task's intermediate features A_F and B_F are passed through a sequence of conv-blocks(W_A and W_B) to compute A_{SF} and B_{SF} according to the following equations:

$$A_{SF_i} = \sigma(W_A \otimes A_{F_i}), \quad (3)$$

$$B_{SF_i} = \sigma(W_B \otimes B_{F_i}). \quad (4)$$

The idea here is to get much more refined features from both tasks before estimating their cross-correlation. The output of this layer preserves the spatial resolution of the input features and gives output features represented by A_{SF} and B_{SF} respectively.

CCAM Sub-block 2: Subsequently in sub-block 2, we build a cross-task relation matrix C_{Mi} for each channel i of A_{SF} , where $C_{Mi} \in \mathbb{R}^{B \times C \times H \times W}$. We then pass the resultant matrix C_{Mi} to a channel attention module Ψ , which estimates the affinity vector α_i between i^{th} channel of A_{SF} and all the channels of B_{SF} in accordance with the equation:

$$\alpha_i = \Psi(A_{SF_i} \otimes (B_{SF})^T), \quad (5)$$

where Ψ denotes a combination of global average pooling layer followed by fully connected layers, with a sigmoid layer at the end. We repeat this for all the channels of A_{SF} to get the corresponding affinity vector α .

CCAM Sub-block 3: As part of sub-block 3, we accumulate *Affinity Scores* for all the channels of A_F to achieve a final cross task affinity matrix M , given by the equation:

$$M = [\alpha_i \oplus \alpha_j] \quad \forall i, j \in [0, C], \quad (6)$$

where \oplus denotes concatenation across the row dimension.

CCAM Sub-block 4: Finally in sub-block 4, the cross task affinity matrix

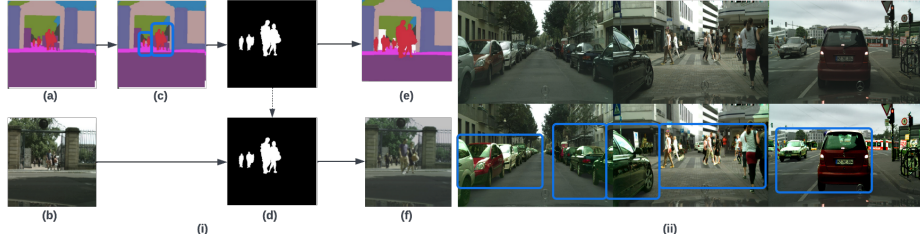


Fig. 3. (i) AffineMix for Semantic Segmentation: Steps involved : (a) GT/ Generated Psuedo label image; (b) Input image; (c) Randomly selected movable object ('Person' class) with random depth scaling of **0.75**; (d) Occlusion aware, affine generated foreground mask; (e) Augmented label image; (f) Augmented Image. (ii) **ColorAug for Depth:** Using intermediate semantics output, purposefully create regions of different brightness, contrast and saturation around movable objects highlighted using blue boxes. Row 1: Original Image, Row 2: Augmented Image.

M achieved serves as a score accumulator, which helps get a linearly weighted features A'_F and B'_F , given by equation:

$$A'_F = A_F + (B_F \odot M), B'_F = B_F + (A_F \odot M^T), \quad (7)$$

where \odot represents element-wise multiplication.

3.3 Data Augmentation

Data augmentation plays a pivotal role in all machine learning tasks, as it helps gather varied data samples from a similar distribution. In the spirit of cooperative multi-tasking, in this subsection, we introduce novel ways of data augmentation both on segmentation and depth estimation tasks using depth and semantics respectively.

Data Augmentation for Segmentation In the context of semi-supervised semantic segmentation, models such as [14, 53, 78] leverage consistency training by mixing image masks across two different images to generate a new image and its semantic labels. Hoyer *et al.* [24] go a step forward to generate a much more diverse mixed label space by maintaining the integrity of the scene structure. We propose a new version of data augmentation called AffineMix, which considers mixing labels within the same image under a varied range of random depth values, thus producing a new set of affine-transformed images (see Fig 3(i)). To further improve the data augmentation process, we mix masks associated with only movable objects, to counter class imbalance, which is stark in a dataset such as Cityscapes. Given an image I and corresponding predicted depth D , we seek to generate a mixed image I' , by scaling the depth of a selected movable object m by a scale factor of s :

$$D' = s * D, \quad (8)$$

such that its spatial location in the image is changed in a geometrically realistic way. Changing the depth by a factor of s , results in an inverse scaling in the

image domain and translational shift which would be given by:

$$t_x = (1.0 - 1/s) * o_x , \quad (9)$$

$$t_y = (1.0 - 1/s) * o_y , \quad (10)$$

where o_x and o_y are normalized offsets along x and y directions. Using t_x , t_y and inverse scaling $1/s$, we can perform affine transformation on the image and label space to generate I_a and L_a . We then estimate the foreground mask, by comparing the new and old depths and masking it with the region which has the movable object in I_a and name it M_m . The final image and label would be then given by:

$$I' = M_m \odot I_a + (1 - M_m) \odot I , \quad (11)$$

$$L' = M_m \odot L_a + (1 - M_m) \odot L . \quad (12)$$

Data Augmentation for Depth As shown in work [17, 74], factors such as position in the image, texture density, shading, and illumination are some of the pictorial cues which give an estimate about distance in a given image. Recent work in this field [11] also re-emphasizes the importance of contrast between adjacent regions as well as bright and dark regions within an image. We particularly leverage this simple albeit important observation to develop a simple yet effective data augmentation technique called ColorAug, which uses different appearance based augmentation on movable and non-movable objects. We use the intermediate semantic labels predicted by the model to guide us in developing such an data augmentation as shown in Fig. 3(ii).

3.4 Self-Supervised Depth

Training formulation of the self-supervised depth network mainly follows good practices of [19] in terms of using a per-pixel minimum appearance, reprojection loss, and an auto-masking strategy. Main backbone of the depth network comprises of an encoder-decoder structure, represented by SE and DD in Fig. 1. We use a subsidiary pose network PN , to predict the relative translation (T) and rotation (R) of the source frames I_{t-1} and I_{t+1} with respect to the target frame I_t . Predicted poses and depth are then used to estimate the self-supervised depth loss, denoted by L_D . Building blocks of the encoder and decoder are specified in more details in Sec. 4.1. We refer the reader to [19] for more details regarding the training strategy.

3.5 Semi-Supervised Semantic Segmentation

For the semi-supervised semantic segmentation module, we start with a set of labeled images Ω_L , the unlabeled images Ω_U , and N unlabeled image sequences. We pretrain the pose network PN , shared encoder SE , and depth decoder DD (see Fig. 1) modules with N unlabeled image sequences, in a similar fashion as mentioned in [24]. During the joint-training step, parameters of the depth decoder (DD) are used to initialize the segmentation decoder (SD) module. The

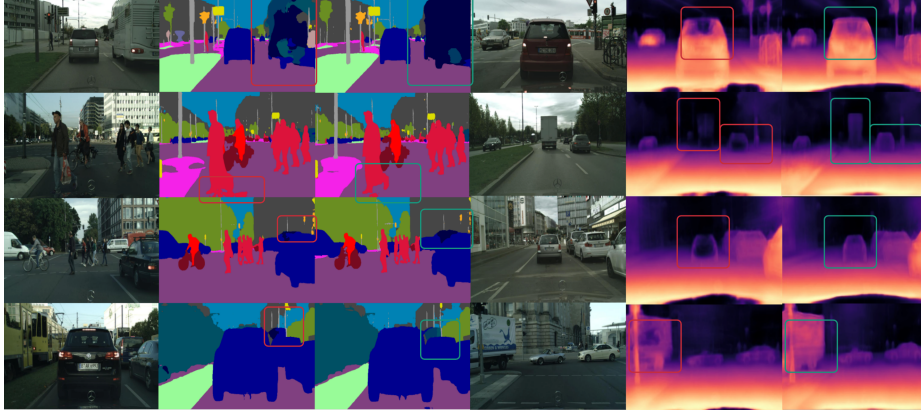


Fig. 4. Qualitative results: In each row we compare the semantics and depth results with the baseline [24]. Red boxes identify shortcomings in the baseline method whereas green boxes highlight the corresponding improvement by using our method.

CCAM module springs into action during this stage of training, facilitating informative features transfer between DD and SD modules. During semi-supervised training, suppose the labeled and unlabeled samples of data is represented as (I_L, S_L) and (I_U, S_U) , where S_U represents pseudo labels, which are generated using a mean teacher algorithm [67]. The parameters of the mean teacher namely θ_T is given by the following equation:

$$\theta'_T = \alpha\theta_T + (1 - \alpha)\theta_{SD} , \quad (13)$$

where θ_{SD} and α represents parameters of the segmentation decoder module, and smoothing coefficient hyper-parameter. We then generate the pseudo labels S_U as suggested in [53] as:

$$S_U = \arg \max_l (\theta_T(I_U)) , \quad (14)$$

where l represents all possible classes in the Cityscapes dataset. Using Eq. (13) and (14), we can formalize the total semi-supervised loss as:

$$L_{SSL} = L_{CE}(\theta_{SD}(I_L), S_L) + L_{CE}(\theta_{SD}(I_U), S_U) . \quad (15)$$

We can now use our AffineMix samples, as a substitute for I_U and S_U in Eq. (15) to get the final semi-supervised loss.

3.6 Orthogonal Regularization (OR)

Orthogonality constraint on model's parameters has shown encouraging results for tasks such as image classification [1, 38, 69], image retrieval [69], 3D classification [55] to name a few. Enforcing orthogonality has also helped improve model's convergence, training stability, and promote learning independent parameters. In a multi-task setup as ours, we share features between the depth and

Model	1/8(372)	1/4(744)	Full(2975)
Adversarial [25]	58.80	62.30	-
s4GAN [50]	59.30	61.90	65.80
DST-CBC [13]	60.50	64.40	-
CutMix [14]	60.34	63.87	67.68
ClassMix [53]	61.25	63.30	-
3-Ways [24]	68.01	69.38	71.16
Ours.	69.98	71.25	72.80

Table 1. Comparative mIoU (in %) numbers on Cityscapes Validation set. Reported numbers are mean over three runs, under same experimental settings.

semantics decoder to facilitate better knowledge transfer between the two tasks. As explained in Sec. 3.2, CCAM module encourages proportional sharing of the feature, by estimating cross channel affinity scores. We postulate that feature independence within a given task is also important. We study the effect of applying a variation of the orthogonal scheme proposed in [1] on different modules, to verify if it does help us to achieve more independent features in a multi-task setup. The new loss function of the model, after adding orthogonal constraint is given by:

$$L_I = L_{SSL} + L_D, \quad (16)$$

$$L_F = L_I + \lambda \cdot \|W^T W - I\|_\sigma, \quad (17)$$

where W , $\|\cdot\|_\sigma$, I , L_F and L_I represents the weights (for each layer), spectral norm, identity matrix, final and initial model loss respectively. As shown in (16), initial model loss consists of semi-supervised segmentation and self-supervised depth loss respectively. We find that enforcing orthogonality, particularly on the parameters of shared encoder SE , depth decoder DD , and segmentation decoder SD has the most positive impact on the model’s performance. We confirm this by calculating average inter-channel correlation, for all decoder layers for both the tasks, with and without OR. In Fig. 5 (ii), we plot the difference between average correlation for four different layers of semantics and depth decoder module, without and with OR. As seen in the plot, we observe a positive difference all along for both semantics and depth modules, suggesting greater inter-channel independence. We postulate that, independent features within semantics and depth module, would make feature transfer between the tasks more effective. Details about enforcing this regularization and ablation study based on this are provided in Sec. 4.1.

4 Experiments

4.1 Experimental Details

Dataset We use the Cityscapes dataset [9] for the training and evaluation of the model. Cityscapes consist of 2975 training and 500 validation images with ground-truth semantic segmentation labels, collected from 21 different European cities. We use the data preprocessing and data augmentation step as suggested

Model	Seg. Metrics	Depth Metrics					
	mIoU \uparrow	AbsRel \downarrow	SqRel \downarrow	RMSE \downarrow	a1 \uparrow	a2 \uparrow	a3 \uparrow
3-ways* [24]	68.09	0.150	2.032	7.492	0.824	0.953	0.985
3-ways* [24] w/o attn	68.07	0.152	2.497	7.621	0.824	0.952	0.982
Ours (CCAM)	69.35	0.142	1.653	7.230	0.824	0.957	0.988
Ours + AM	69.64	0.149	1.852	7.562	0.815	0.952	0.986
Ours + AM + OR	69.98	0.146	1.573	7.331	0.817	0.953	0.987
Ours + AM + OR + CA	69.98	0.142	1.553	7.284	0.824	0.956	0.987

Table 2. Comparative mIoU and depth results between baseline model with (vanilla) attention, without attention, and with cross channel affinity attention. Models with * show the results as reproduced by us running the original model. AM: AffineMix, OR: orthogonal Regularization, CA: ColorAug.

Metric	CutOut	CutMix	ClassMix	DepthMix	AffineMix
mIoU	57.74	60.34	63.86	68.09	68.70

Table 3. Table presents the comparative performance of AffineMix method with previous semi-supervised works, which establishes AffineMix superiority over previous approaches on Cityscapes dataset(1/8 labeled images).

in [24], where we firstly downsample the original color images from 2048x1024 to 1024x512, which are furthered center-cropped to get final image size to 512x512 for training. For semi-supervised segmentation, we use only 2975 labeled training images, which are randomly split into a labeled and an unlabeled subset. For depth we use the unlabeled frames provided by the Cityscapes dataset during the training phase, whereas depth is evaluated against 1525 images from 6 cities taken from the test set, for which we use the ground-truth depths generated by Watson *et al.* in [72], using the disparity maps provided by Cityscapes.

Network Architecture Basic network as part of our multi-task training is similar to [24, 76] as seen in Fig. 1(a), which provides an intuitive and effective network for simultaneous training. It comprises of a shared encoder network which is ResNet101 [22] with output stride as 16. We use two different decoder modules for semantics and depth respectively, which is a combination of Deeplabv3 [3] with a U-Net [58] decoder. ASPP Blocks [22] with dilation rates of 6, 12 and 18 are used for aggregating encoder features of different scales. U-Net [58] decoder has five upsampling blocks with skip connections, with output channel as 256, 256, 128, 128 and 64 respectively. For pose network we use ResNet18 [22] as encoder network, whereas for the encoder network we use ResNet101 [22] pretrained on the ImageNet dataset [60]. We refer the reader to the original paper’s [24] supplementary section for more details. CCAM block consists of two convolutional blocks with kernel size of 3x3 and padding of 1, followed by a sigmoid layer, for the spatial attention. For the channel attention layer, intermediate output features are then passed through a global average layer, and two fully connected layers which first reduces channel by 2 and then brings back to original number of channels. It is then followed by a sigmoid layer to generate the affinity matrix for each channel. Further details about CCAM block architecture is provided in suppl. material.

Training For most part of the training, we follow the procedure as mentioned by Hoyer *et al.* [24]. We first train the self-supervised depth and pose module

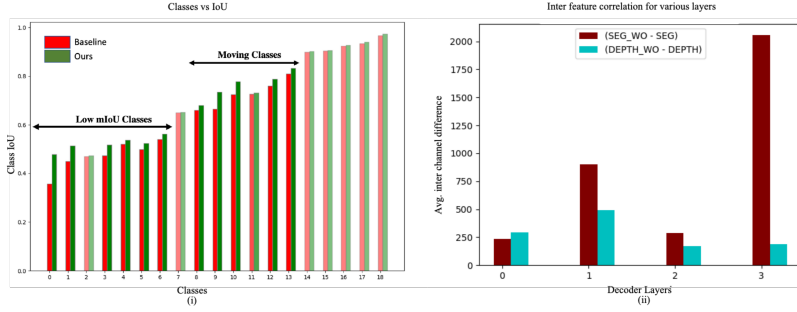


Fig. 5. (i) **Class Specific mIoU:** Comparative improvement in IoU numbers in increasing order. (ii) Figure shows the difference between the average correlation between all features for semantics and depth decoder, for without (WO) OR and with OR.

alone using Adam [30] till 300K iterations, with an initial learning rate of 10^{-4} , which is reduced by a factor of 10 using the step-scheduled learning rate mechanism. In the second iteration we only look to fine-tune the shared encoder with a ImageNet feature distance for another 50K iterations. During joint training, we use SGD with an initial learning rate of 10^{-3} and 10^{-2} for encoder and decoder respectively, which is reduced by a factor of 10 after 30K iterations. The whole model is trained for a total of 40K iterations. We also use a momentum of 0.9, weight decay of 5×10^{-4} , and a gradient norm clipping of 10 for the optimizer. We further use a mean teacher with $\alpha = 0.99$, which is predominantly used during self-supervised semantic training. We find freezing depth decoder parameters during data augmentation steps of self-supervised semantic learning, leads to better model stability, without any adverse effect on semantics or depth results. For orthogonal regularization we follow an approach similar to one suggested by Bansal *et al.* [1], starting with an orthogonal weight $\lambda_O = 10^{-4}$, which is then reduced gradually to 10^{-5} , 10^{-6} and 10^{-7} after 10K, 20K and 30K iterations respectively.

4.2 Ablation

Cross Channel Affinity Block We start with studying the effectiveness of the self-attention distillation module used in baseline [24] for cross-feature transfer between depth and semantics tasks. We follow that up with an experiment, incorporating the CCAM module as shown in Fig. 1(a) and validate its positive impact on both tasks. As seen in Tab. 2, we observe minimal improvement to semantics and depth metrics with and without self-attention based distillation module; with mean IoU and absolute relative errors hover around 68% and 15%. Including just CCAM module, we see an improvement of **1.28%** in mIoU and a drop of **5.3%** in the absolute relative depth error. We further incorporate the proposed AffineMix data augmentation, mainly with an aim to improve on semi-supervised semantic segmentation training. Through our experiments, we find that AffineMix consistently improves upon the baseline by **1.74%** respectively as shown in Tab. 2. We see a drop in the depth metrics after applying AffineMix. We postulate this drop in depth performance is due to visual incoherence in the

local region adjoining to newly added objects, which might be detrimental to the depth task. We precisely overcome this limitation by using ColorAug that help us achieve back the 14.2% absolute relative error for the depth task.

Orthogonal Regularization For verifying the efficacy of OR (Fig. 1(b)), we start out by comparing models trained with and without OR, from the perspective of feature independence after the completion of training. As postulated, we find that the features across all 4 layers of depth and semantics (decoder) module are much more independent after applying such a regularization. We measure this by calculating the cross-correlation between the features of depth and semantics separately before and after applying OR. Results achieved always have a positive difference for average correlation for both depth and semantics module between without OR and with OR model as seen in Fig. 5(ii). We further validate this claim by seeing a consistent improvement in semantics and depth metrics. We see an average gain of about **0.34%** over a run of three experiments for AffineMix augmentation, and an improvement of about **1.89%** compared to the baseline model. We also observe a marginal boost to depth metrics after inclusion of OR by **2.01%**(see Tab. 2).

AffineMix Augmentation We did a comparative ablation experiment verifying the efficacy of proposed data augmentation with the previous data augmentation approaches. As shown in Table. 3, we observe an improvement of about 8.36, 4.64 and 0.61 in mIoU numbers when compared to [24, 53, 78] respectively.

ColorAug Augmentation For the depth augmentation experiment, we leverage the intermediate semantics information to create a new set of images, which helps us create regions of different contrast, brightness, and saturation around movable objects. We use this data augmentation scheme only after 10K steps of training, such that semantic outputs from the network are reliable to some extent ($\text{mIoU} \geq 60\%$). We achieve a reduction of about 2.8% to reach an absolute relative error of **14.2%** as seen in Tab. 2.

Overall, we achieve improvements of about **1.89%**, **1.87%**, **1.64%** for semantic metrics for 372, 744 and 2975 samples of Cityscapes dataset respectively, when compared with its previous best performing counterpart in a joint training paradigm. Using our training strategy, we parallelly improve the depth metrics by **5.3%**. Diving deep a bit, we took a closer look to narrow down the classes, which are most positively impacted by our training strategy. For this we plot mIoU numbers in an increasing order ³, and find that much of improvement is mainly seen for *low-mIoU-classes* such as motorcycle, wall, rider and *movable-classes* such as bicycle, train, truck and bus, whereas *saturated-class* such as building, vegetation, car, sky and road shows marginal improvements as these classes already have achieved about 90% mIoU.

³ Order: motorcycle, wall, fence, rider, pole, traffic-light, terrain, traffic-sign, bicycle, train, truck, person, sidewalk, bus, building, vegetation, car, sky, road.

5 Conclusions

Through this paper, we take forward the legacy of multi-task learning to the next step and show that two complementary tasks can be gelled together to mutually help each other. In this work, we successfully establish, how effective transfer of features between semantics and depth estimation modules, could result in substantial performance gain for both depth and semantics tasks. Building such a model yields further gain when followed up with an intelligent and diverse data augmentation for both depth and semantics. We hope encouraging results seen through our work would further push the research community in working towards finding much more efficient and effective ways for multi-task learning.

References

1. Bansal, N., Chen, X., Wang, Z.: Can we gain more from orthogonality regularizations in training deep cnns? arXiv preprint arXiv:1810.09102 (2018)
2. Caruana, R.: Multitask learning. *Machine learning* **28**(1), 41–75 (1997)
3. Chen, L.C., Papandreou, G., Kokkinos, I., Murphy, K., Yuille, A.L.: Deeplab: Semantic image segmentation with deep convolutional nets, atrous convolution, and fully connected crfs. *IEEE Transactions on Pattern Analysis and Machine Intelligence* **40**(4), 834–848 (2017)
4. Chen, L.C., Papandreou, G., Schroff, F., Adam, H.: Rethinking atrous convolution for semantic image segmentation. arXiv preprint arXiv:1706.05587 (2017)
5. Chen, L.C., Yang, Y., Wang, J., Xu, W., Yuille, A.L.: Attention to scale: Scale-aware semantic image segmentation. In: *Proceedings of the IEEE Conference on Computer Vision and Pattern Recognition*. pp. 3640–3649 (2016)
6. Chen, L.C., Zhu, Y., Papandreou, G., Schroff, F., Adam, H.: Encoder-decoder with atrous separable convolution for semantic image segmentation. In: *Proceedings of the European Conference on Computer Vision*. pp. 801–818 (2018)
7. Chen, P.Y., Liu, A.H., Liu, Y.C., Wang, Y.C.F.: Towards scene understanding: Unsupervised monocular depth estimation with semantic-aware representation. In: *Proceedings of the IEEE/CVF Conference on Computer Vision and Pattern Recognition* (June 2019)
8. Chen, Z., Badrinarayanan, V., Lee, C.Y., Rabinovich, A.: Gradnorm: Gradient normalization for adaptive loss balancing in deep multitask networks. In: *International Conference on Machine Learning*. pp. 794–803. PMLR (2018)
9. Cordts, M., Omran, M., Ramos, S., Rehfeld, T., Enzweiler, M., Benenson, R., Franke, U., Roth, S., Schiele, B.: The cityscapes dataset for semantic urban scene understanding. In: *Proceedings of the IEEE Conference on Computer Vision and Pattern Recognition*. pp. 3213–3223 (2016)
10. Dai, J., He, K., Sun, J.: Convolutional feature masking for joint object and stuff segmentation. In: *Proceedings of the IEEE Conference on Computer Vision and Pattern Recognition*. pp. 3992–4000 (2015)
11. Dijk, T.v., Croon, G.d.: How do neural networks see depth in single images? In: *Proceedings of the IEEE/CVF International Conference on Computer Vision*. pp. 2183–2191 (2019)
12. Farabet, C., Couprie, C., Najman, L., LeCun, Y.: Learning hierarchical features for scene labeling. *IEEE Transactions on Pattern Analysis and Machine Intelligence* **35**(8), 1915–1929 (2012)

13. Feng, Z., Zhou, Q., Gu, Q., Tan, X., Cheng, G., Lu, X., Shi, J., Ma, L.: Dmt: Dynamic mutual training for semi-supervised learning. arXiv preprint arXiv:2004.08514 (2020)
14. French, G., Laine, S., Aila, T., Mackiewicz, M., Finlayson, G.: Semi-supervised semantic segmentation needs strong, varied perturbations. arXiv preprint arXiv:1906.01916 (2019)
15. Gao, Y., Ma, J., Zhao, M., Liu, W., Yuille, A.L.: Nddr-cnn: Layerwise feature fusing in multi-task cnns by neural discriminative dimensionality reduction. In: Proceedings of the IEEE/CVF Conference on Computer Vision and Pattern Recognition. pp. 3205–3214 (2019)
16. Garg, R., Bg, V.K., Carneiro, G., Reid, I.: Unsupervised cnn for single view depth estimation: Geometry to the rescue. In: European Conference on Computer Vision. pp. 740–756. Springer (2016)
17. Gibson, J.J.: The perception of the visual world. (1950)
18. Godard, C., Mac Aodha, O., Brostow, G.J.: Unsupervised monocular depth estimation with left-right consistency. In: Proceedings of the IEEE Conference on Computer Vision and Pattern Recognition. pp. 270–279 (2017)
19. Godard, C., Mac Aodha, O., Firman, M., Brostow, G.J.: Digging into self-supervised monocular depth estimation. In: Proceedings of the IEEE/CVF International Conference on Computer Vision. pp. 3828–3838 (2019)
20. Guizilini, V., Hou, R., Li, J., Ambrus, R., Gaidon, A.: Semantically-guided representation learning for self-supervised monocular depth. arXiv preprint arXiv:2002.12319 (2020)
21. Guo, M., Haque, A., Huang, D.A., Yeung, S., Fei-Fei, L.: Dynamic task prioritization for multitask learning. In: Proceedings of the European conference on computer vision (ECCV). pp. 270–287 (2018)
22. He, K., Zhang, X., Ren, S., Sun, J.: Deep residual learning for image recognition. In: Proceedings of the IEEE Conference on Computer Vision and Pattern Recognition. pp. 770–778 (2016)
23. Heuer, F., Mantowsky, S., Bukhari, S., Schneider, G.: Multitask-centernet (mcn): Efficient and diverse multitask learning using an anchor free approach. In: Proceedings of the IEEE/CVF International Conference on Computer Vision. pp. 997–1005 (2021)
24. Hoyer, L., Dai, D., Chen, Y., Koring, A., Saha, S., Van Gool, L.: Three ways to improve semantic segmentation with self-supervised depth estimation. In: Proceedings of the IEEE/CVF Conference on Computer Vision and Pattern Recognition. pp. 11130–11140 (2021)
25. Hung, W.C., Tsai, Y.H., Liou, Y.T., Lin, Y.Y., Yang, M.H.: Adversarial learning for semi-supervised semantic segmentation. arXiv preprint arXiv:1802.07934 (2018)
26. Ji, P., Li, R., Bhanu, B., Xu, Y.: Monoindoor: Towards good practice of self-supervised monocular depth estimation for indoor environments. In: Proceedings of the IEEE/CVF International Conference on Computer Vision. pp. 12787–12796 (2021)
27. Ji, P., Yan, Q., Ma, Y., Xu, Y.: Georefine: Self-supervised online depth refinement for accurate dense mapping. arXiv preprint arXiv:2205.01656 (2022)
28. Jiao, J., Cao, Y., Song, Y., Lau, R.: Look deeper into depth: Monocular depth estimation with semantic booster and attention-driven loss. In: Proceedings of the European Conference on Computer Vision (September 2018)
29. Kendall, A., Gal, Y., Cipolla, R.: Multi-task learning using uncertainty to weigh losses for scene geometry and semantics. In: Proceedings of the IEEE Conference on Computer Vision and Pattern Recognition. pp. 7482–7491 (2018)

30. Kingma, D.P., Ba, J.: Adam: A method for stochastic optimization. arXiv preprint arXiv:1412.6980 (2014)
31. Klingner, M., Termöhlen, J.A., Mikolajczyk, J., Fingscheidt, T.: Self-supervised monocular depth estimation: Solving the dynamic object problem by semantic guidance. In: European Conference on Computer Vision. pp. 582–600. Springer (2020)
32. Kokkinos, I.: Ubertnet: Training a universal convolutional neural network for low-, mid-, and high-level vision using diverse datasets and limited memory. In: Proceedings of the IEEE conference on computer vision and pattern recognition. pp. 6129–6138 (2017)
33. Laine, S., Aila, T.: Temporal ensembling for semi-supervised learning. arXiv preprint arXiv:1610.02242 (2016)
34. LeCun, Y., Bottou, L., Bengio, Y., Haffner, P.: Gradient-based learning applied to document recognition. *Proceedings of the IEEE* **86**(11), 2278–2324 (1998)
35. Lee, J., Kim, E., Lee, S., Lee, J., Yoon, S.: Ficklenet: Weakly and semi-supervised semantic image segmentation using stochastic inference. In: Proceedings of the IEEE/CVF Conference on Computer Vision and Pattern Recognition. pp. 5267–5276 (2019)
36. Li, H., Xiong, P., An, J., Wang, L.: Pyramid attention network for semantic segmentation. arXiv preprint arXiv:1805.10180 (2018)
37. Li, K., Wu, Z., Peng, K.C., Ernst, J., Fu, Y.: Tell me where to look: Guided attention inference network. In: Proceedings of the IEEE Conference on Computer Vision and Pattern Recognition. pp. 9215–9223 (2018)
38. Li, S., Jia, K., Wen, Y., Liu, T., Tao, D.: Orthogonal deep neural networks. *IEEE Transactions on Pattern Analysis and Machine Intelligence* **43**(4), 1352–1368 (2021). <https://doi.org/10.1109/TPAMI.2019.2948352>
39. Lin, G., Milan, A., Shen, C., Reid, I.: Refinenet: Multi-path refinement networks for high-resolution semantic segmentation. In: Proceedings of the IEEE Conference on Computer Vision and Pattern Recognition. pp. 1925–1934 (2017)
40. Lin, G., Shen, C., Van Den Hengel, A., Reid, I.: Efficient piecewise training of deep structured models for semantic segmentation. In: Proceedings of the IEEE Conference on Computer Vision and Pattern Recognition. pp. 3194–3203 (2016)
41. Liu, J., Ji, P., Bansal, N., Cai, C., Yan, Q., Huang, X., Xu, Y.: Planemvs: 3d plane reconstruction from multi-view stereo. In: Proceedings of the IEEE/CVF Conference on Computer Vision and Pattern Recognition. pp. 8665–8675 (2022)
42. Liu, S., Johns, E., Davison, A.J.: End-to-end multi-task learning with attention. In: Proceedings of the IEEE/CVF Conference on Computer Vision and Pattern Recognition. pp. 1871–1880 (2019)
43. Liu, S., Johns, E., Davison, A.J.: End-to-end multi-task learning with attention. In: Proceedings of the IEEE/CVF conference on computer vision and pattern recognition. pp. 1871–1880 (2019)
44. Liu, W., Rabinovich, A., Berg, A.C.: Parsenet: Looking wider to see better. arXiv preprint arXiv:1506.04579 (2015)
45. Long, J., Shelhamer, E., Darrell, T.: Fully convolutional networks for semantic segmentation. In: Proceedings of the IEEE Conference on Computer Vision and Pattern Recognition. pp. 3431–3440 (2015)
46. Long, M., Cao, Z., Wang, J., Yu, P.S.: Learning multiple tasks with multilinear relationship networks. *Advances in neural information processing systems* **30** (2017)
47. Maninis, K.K., Radosavovic, I., Kokkinos, I.: Attentive single-tasking of multiple tasks. In: Proceedings of the IEEE/CVF Conference on Computer Vision and Pattern Recognition. pp. 1851–1860 (2019)

48. Misra, I., Shrivastava, A., Gupta, A., Hebert, M.: Cross-stitch networks for multi-task learning. In: Proceedings of the IEEE conference on computer vision and pattern recognition. pp. 3994–4003 (2016)
49. Misra, I., Shrivastava, A., Gupta, A., Hebert, M.: Cross-stitch networks for multi-task learning. In: Proceedings of the IEEE Conference on Computer Vision and Pattern Recognition. pp. 3994–4003 (2016)
50. Mittal, S., Tatarchenko, M., Brox, T.: Semi-supervised semantic segmentation with high-and low-level consistency. *IEEE Transactions on Pattern Analysis and Machine Intelligence* (2019)
51. Miyato, T., Maeda, S.i., Koyama, M., Ishii, S.: Virtual adversarial training: a regularization method for supervised and semi-supervised learning. *IEEE Transactions on Pattern Analysis and Machine Intelligence* **41**(8), 1979–1993 (2018)
52. Mnih, V., Heess, N., Graves, A., et al.: Recurrent models of visual attention. In: *Advances in Neural Information Processing Systems*. pp. 2204–2212 (2014)
53. Olsson, V., Tranheden, W., Pinto, J., Svensson, L.: Classmix: Segmentation-based data augmentation for semi-supervised learning. In: *Proceedings of the IEEE/CVF Winter Conference on Applications of Computer Vision*. pp. 1369–1378 (2021)
54. Ouali, Y., Hudelot, C., Tami, M.: Semi-supervised semantic segmentation with cross-consistency training. In: *Proceedings of the IEEE/CVF Conference on Computer Vision and Pattern Recognition*. pp. 12674–12684 (2020)
55. Qi, C.R., Su, H., Mo, K., Guibas, L.J.: Pointnet: Deep learning on point sets for 3d classification and segmentation. In: *Proceedings of the IEEE Conference on Computer Vision and Pattern Recognition*. pp. 652–660 (2017)
56. Ramirez, P.Z., Poggi, M., Tosi, F., Mattoccia, S., Di Stefano, L.: Geometry meets semantics for semi-supervised monocular depth estimation. In: *Asian Conference on Computer Vision*. pp. 298–313. Springer (2018)
57. Rebuffi, S.A., Bilen, H., Vedaldi, A.: Learning multiple visual domains with residual adapters. *Advances in neural information processing systems* **30** (2017)
58. Ronneberger, O., Fischer, P., Brox, T.: U-net: Convolutional networks for biomedical image segmentation. In: *International Conference on Medical Image Computing and Computer-Assisted Intervention*. pp. 234–241. Springer (2015)
59. Ruder, S., Bingel, J., Augenstein, I., Søgaard, A.: Latent multi-task architecture learning. In: *Proceedings of the AAAI Conference on Artificial Intelligence*. vol. 33, pp. 4822–4829 (2019)
60. Russakovsky, O., Deng, J., Su, H., Krause, J., Satheesh, S., Ma, S., Huang, Z., Karpathy, A., Khosla, A., Bernstein, M., Berg, A.C., Fei-Fei, L.: ImageNet Large Scale Visual Recognition Challenge. *International Journal of Computer Vision* **115**(3), 211–252 (2015). <https://doi.org/10.1007/s11263-015-0816-y>
61. Sener, O., Koltun, V.: Multi-task learning as multi-objective optimization. *Advances in neural information processing systems* **31** (2018)
62. Sermanet, P., Eigen, D., Zhang, X., Mathieu, M., Fergus, R., LeCun, Y.: Overfeat: Integrated recognition, localization and detection using convolutional networks. *arXiv preprint arXiv:1312.6229* (2013)
63. Shinohara, Y.: Adversarial Multi-Task Learning of Deep Neural Networks for Robust Speech Recognition. In: *Proc. Interspeech 2016*. pp. 2369–2372 (2016). <https://doi.org/10.21437/Interspeech.2016-879>
64. Sinha, A., Chen, Z., Badrinarayanan, V., Rabinovich, A.: Gradient adversarial training of neural networks. *arXiv preprint arXiv:1806.08028* (2018)
65. Standley, T., Zamir, A., Chen, D., Guibas, L., Malik, J., Savarese, S.: Which tasks should be learned together in multi-task learning? In: *International Conference on Machine Learning*. pp. 9120–9132. PMLR (2020)

66. Sun, X., Panda, R., Feris, R., Saenko, K.: Adashare: Learning what to share for efficient deep multi-task learning. arXiv preprint arXiv:1911.12423 (2019)
67. Tarvainen, A., Valpola, H.: Mean teachers are better role models: Weight-averaged consistency targets improve semi-supervised deep learning results. arXiv preprint arXiv:1703.01780 (2017)
68. Tiwari, L., Ji, P., Tran, Q.H., Zhuang, B., Anand, S., Chandraker, M.: Pseudo rgb-d for self-improving monocular slam and depth prediction. In: European conference on computer vision. pp. 437–455 (2020)
69. Wang, J., Chen, Y., Chakraborty, R., Yu, S.X.: Orthogonal convolutional neural networks. In: Proceedings of the IEEE/CVF Conference on Computer Vision and Pattern Recognition (June 2020)
70. Wang, X., Girshick, R., Gupta, A., He, K.: Non-local neural networks. In: Proceedings of the IEEE Conference on Computer Vision and Pattern Recognition. pp. 7794–7803 (2018)
71. Wang, Y., Zhang, J., Kan, M., Shan, S., Chen, X.: Self-supervised equivariant attention mechanism for weakly supervised semantic segmentation. In: Proceedings of the IEEE/CVF Conference on Computer Vision and Pattern Recognition. pp. 12275–12284 (2020)
72. Watson, J., Mac Aodha, O., Prisacariu, V., Brostow, G., Firman, M.: The temporal opportunist: Self-supervised multi-frame monocular depth. In: Proceedings of the IEEE/CVF Conference on Computer Vision and Pattern Recognition. pp. 1164–1174 (2021)
73. Wei, Y., Xiao, H., Shi, H., Jie, Z., Feng, J., Huang, T.S.: Revisiting dilated convolution: A simple approach for weakly-and semi-supervised semantic segmentation. In: Proceedings of the IEEE Conference on Computer Vision and Pattern Recognition. pp. 7268–7277 (2018)
74. Wixted, J.T., Thompson-Schill, S.L.: Stevens’ Handbook of Experimental Psychology and Cognitive Neuroscience, Language and Thought, vol. 3. John Wiley & Sons (2018)
75. Xie, Q., Dai, Z., Hovy, E., Luong, M.T., Le, Q.V.: Unsupervised data augmentation for consistency training. arXiv preprint arXiv:1904.12848 (2019)
76. Xu, D., Ouyang, W., Wang, X., Sebe, N.: Pad-net: Multi-tasks guided prediction-and-distillation network for simultaneous depth estimation and scene parsing. In: Proceedings of the IEEE Conference on Computer Vision and Pattern Recognition. pp. 675–684 (2018)
77. Yu, F., Koltun, V.: Multi-scale context aggregation by dilated convolutions. arXiv preprint arXiv:1511.07122 (2015)
78. Yun, S., Han, D., Oh, S.J., Chun, S., Choe, J., Yoo, Y.: Cutmix: Regularization strategy to train strong classifiers with localizable features. In: Proceedings of the IEEE/CVF International Conference on Computer Vision. pp. 6023–6032 (2019)
79. Zhang, Y., Yang, Q.: A survey on multi-task learning. IEEE Transactions on Knowledge and Data Engineering (2021)
80. Zhang, Z., Cui, Z., Xu, C., Yan, Y., Sebe, N., Yang, J.: Pattern-affinitive propagation across depth, surface normal and semantic segmentation. In: Proceedings of the IEEE/CVF Conference on Computer Vision and Pattern Recognition. pp. 4106–4115 (2019)
81. Zhao, H., Shi, J., Qi, X., Wang, X., Jia, J.: Pyramid scene parsing network. In: Proceedings of the IEEE Conference on Computer Vision and Pattern Recognition. pp. 2881–2890 (2017)

- 82. Zhou, B., Khosla, A., Lapedriza, A., Oliva, A., Torralba, A.: Learning deep features for discriminative localization. In: Proceedings of the IEEE Conference on Computer Vision and Pattern Recognition. pp. 2921–2929 (2016)
- 83. Zhou, T., Brown, M., Snavely, N., Lowe, D.G.: Unsupervised learning of depth and ego-motion from video. In: Proceedings of the IEEE Conference on Computer Vision and Pattern Recognition. pp. 1851–1858 (2017)
- 84. Zou, Y., Ji, P., Tran, Q.H., Huang, J.B., Chandraker, M.: Learning monocular visual odometry via self-supervised long-term modeling. In: European Conference on Computer Vision. pp. 710–727 (2020)